Journal of Pharmaceutical and Biomedical Analysis 49 (2009) 338–346

Contents lists available at ScienceDirect

Journal of Pharmaceutical and Biomedical Analysis

journal homepage: www.elsevier.com/locate/jpba

Quantitative determination of famotidine polymorphs: X-ray powder diffractometric and Raman spectrometric study

Zoltán Német[a], Győző Csonka Kis[a], György Pokol[b], Ádám Demeter[a,*]

[a] Drug Polymorphism Research Division, Gedeon Richter Plc., P.O. Box 27, H-1475 Budapest, Hungary
[b] Department of Inorganic and Analytical Chemistry, Budapest University of Technology and Economics, Szt. Gellért tér 4, H-1111 Budapest, Hungary

ARTICLE INFO

Article history:
Received 7 August 2008
Received in revised form
12 November 2008
Accepted 27 November 2008
Available online 3 December 2008

Keywords:
X-ray powder diffractometry
Raman spectrometry
Quantitative analysis
Multivariate calibration
Famotidine polymorphs

ABSTRACT

X-ray powder diffractometric and Raman spectrometric methods were developed for quantitative measurement of the polymorphic forms of famotidine in their mixtures. This study aims to deduce some useful conclusions regarding quantitative polymorph analysis, which could also be utilized in industrial practice. Both form A and form B of famotidine possess specific X-ray diffraction reflections as well as characteristic Raman vibrational bands, which permits simple determination of the phases in their mixtures. Keeping in mind that multivariate data processing by chemometric approach is thought of nowadays as superior over univariate one, the results of the two evaluation methods were compared by precision, accuracy as well as robustness. It was found that both approaches provide similar results provided analytically useful data regions are properly selected. Overcoming the common problems of quantitative X-ray powder diffractometry and solid state Raman spectrometry both permit accurate quantification of famotidine polymorphs; the latter, however, seems to be more favourable in regular laboratory practice.

1. Introduction

The frequent occurrence of polymorphism of pharmaceutical solids is known for a long time past; as well as the fact that different polymorphic forms of active ingredients may have different bioavailability [1]. Because of the regulatory constraints of the last few decades, which force pharmaceutical companies to deal with polymorphism of active ingredients [2,3], and even more for the economic potential of its new solid forms [4,5], the relevance of the pharmaceutical polymorph analysis is constantly growing. This is evidenced by many excellent recent publications, which discuss the subject in detail [4,6–8]. The importance of quantitative solid state analysis in polymorph research is also increasing; practically for two reasons. Detection of low level of unwanted solid forms in the developed one is required from quality assurance point of view, provided that bioavailability is affected by polymorphism [3]. Measurement of the polymorph composition can only be accomplished via sensitive solid state analytical techniques, which provides a firm basis for a better in-process technological control over undesired polymorph transitions. The second reason arises from patent infringement aspects. On account of a specific patent right situation a generic manufacturer may have no other choice to enter the market with a formulation which contains the active ingredient as a polymorphic mixture of two solid forms. In this case, determination of the polymorph composition is a constraint from both quality assurance and patent point of view.

X-ray powder diffraction (XRPD) has been used for quantitative phase analysis for almost a century. It is based on direct proportionality of intensity of the reflection with the weight fraction of the phase which it is characteristic for [9]. The technique was also successfully utilized for the quantitative measurement of pharmaceutical substances [10–18]. As a novel approach, whole powder pattern fitting methods [19–21] are spreading, which permit more accurate and precise quantitation, since these are less sensitive for experimental errors concerning the sample properties and preparation, especially preferred orientation.

It is also well known that Raman spectroscopy can be used for quantitative analysis. A recent publication reviews the potential and limitations of the technique, as well as reports many examples, in which it was successfully applied [22]. Two other thorough reviews deal specially with pharmaceutical applications of Raman spectroscopy, including quantitative analytical aspects as well [23,24]. There are some good examples when the authors used univariate calibration to quantify the polymorph content [25–29]. Multivariate calibrations, utilizing more spectral information than a single height or integrated intensity of a vibrational band, are usually applied if the spectral differences are relatively small; hence the accurate measurement of the previous quantities is not possible [30–35].

* Corresponding author. Tel.: +36 1 431 5922; fax: +36 1 432 6006.
E-mail address: a.demeter@richter.hu (Á. Demeter).

0731-7085/$ – see front matter © 2008 Elsevier B.V. All rights reserved.
doi:10.1016/j.jpba.2008.11.033

The aim of this study was to develop a suitable solid state analytical method for measuring the polymorph composition of famotidine applicable in routine laboratory practice in the pharmaceutical industry. Famotidine is a widely used histamine H_2-receptor antagonist having two polymorphic forms: the thermodynamically stable form A and the kinetically favoured form B [36]. The substance is a typical example of conformational polymorphism [37], hence not only the X-ray powder diffraction patterns of two forms are very different, but their vibrational spectra as well.

There is no publication presented so far dealing with quantification of the relative amount of famotidine polymorphs. Preliminary experiments indicated that infrared spectroscopy is very sensitive for the detection of form B due to the appearance of its sharp band at 3506 cm^{-1}. This allows detection of form B down to 1% in a polymorphic mixture. Further efforts with FT-IR spectrometry, however, did not succeed in establishing usable calibration correlation in the concentration range of 0–100%, either in transmission mode in potassium bromide pellet or with diffuse reflection technique. As the melting points of the polymorphs are rather different, in spite of the rapid decomposition of the substance during melting, the melting enthalpies can be measured by a proper DSC method. The technique has, however, a considerable drawback in a quantitative analysis, as it was shown that the apparent enthalpies are also the function of mechanical activation which affected the sample before the measurement [38]. Therefore DSC analysis does not unequivocally reflect the true composition of famotidine polymorphic mixtures.

There are distinct X-ray diffraction reflections and also unique Raman bands of both famotidine polymorphs, indicating that these two powerful solid state analytical techniques are appropriate for quantitative purposes. Univariate and multivariate calibrations were performed on both XRPD and Raman data sets with different multivariate methods and spectral processing procedures, and the two techniques were compared from practical industrial laboratory aspects. This comparison is similar to that published recently about the quantitative analysis of carbamazepine anhydrate and dihydrate [39].

2. Materials and methods

2.1. Materials

Famotidine form A and form B were obtained from a synthetic laboratory in the manufacturing plant of Gedeon Richter Plc. Both forms were of high chemical purity (greater than 99.5% determined by HPLC), and were also phase-pure according to XRPD, Raman and DSC measurements. Famotidine polymorphic mixtures of unknown composition were crystallized under different conditions.

2.2. Preparation of polymorphic mixtures

Binary polymorphic mixtures containing 1, 2, 5, 8, 10, 15, 20, 30, 50, 70, 80, 85, 90, 92, 95, 98, 99 and 100% of form A were prepared with a similar procedure previously proposed by other authors [12]: suspending accurately weighted amounts of two forms in hexane with stirring for 40 min, in 10 g scale. Validation mixtures containing 3, 7, 11, 89, 93 and 97% of form A were prepared in the same way. These mixtures were not incorporated into calibration models, but used for assessing their validity.

To produce ground samples 0.5 g of calibration and validation mixtures were gently ground in agate mortar with a pestle for 3 min.

2.3. FT-Raman spectrometry

Raman spectra were collected by Thermo Nicolet NXR-9650 FT-Raman spectrometer equipped with Nd-YAG laser source at 1064 nm wavelength, liquid nitrogen cooled Ge detector and MicroStage™ with laser spot focused on 50 μm. After careful preliminary investigations regarding the maximum tolerable laser power and exposure time, as well as homogeneity problems, four scans were co-added from 25 different positions of the sample at 500 mW exciting power and 4 cm^{-1} spectral resolution. Samples were filled into the holes of a home-made sample holder accessory [40], which allowed defining a 2.5 mm × 2.5 mm area with 25 equidistant points on a smooth, compact sample surface. Data collection was performed by Thermo Nicolet Omnic software, version 7.2.

2.4. X-ray powder diffractometry

Diffraction patterns were measured on PANalytical X'Pert PRO diffractometer using Cu Kα radiation with 40 kV accelerating voltage and 40 mA anode current at a scanning rate of 0.031° 2θ min^{-1} over the range of 10–34° 2θ with 0.013° step size in reflection mode, spinning the sample holder by 1 s^{-1}. PIXcel detector was used with 0.04 sollers; automatic divergence and antiscatter slits were set to 10 mm constant irradiated length. About 0.5 g of samples was filled from the back into the circular stainless steel sample holder and pressed against metal plate to give compact and smooth surface. Every sample was measured in triplicate, filling another portion of the mixture into the sample holder; except for ground samples, which were repacked in the sample holder. Data were collected by PANalytical Data Collector, version 2.2.

2.5. Data analysis

Univariate data analysis was performed by Omnic software and Microsoft Excel. Diffractograms were converted into jcamp format before the evaluation, and were treated the same way as Raman spectra.

Multivariate data analysis was carried out by Thermo Nicolet TQ Analyst 7.2 software. Classical least squares (CLS), principal component regression (PCR) and partial least squares (PLS) methods were tested with different path length types and spectral preprocessing steps on different spectral ranges.

The results of different data processing procedures were compared using linear correlation coefficients (r), root-mean-squared errors of calibration (RMSEC), cross-validation (RMSECV) and prediction (RMSEP) values. These are defined by the following equation:

$$\mathrm{RMSE} = \sqrt{\frac{\sum_{i=1}^{n}(y_i - Y_i)^2}{n}},$$

where y_i, Y_i and n are the calculated value, the theoretical value (neglecting the possibility of inaccurate mixture preparation, this was considered equal to the nominal value) and the number of measurements, respectively, for calibration, cross-validation and prediction.

3. Results and discussion

3.1. X-ray powder diffractometry

The basic equation which permits the quantitative analytical application of X-ray powder diffraction is $I_p = K_p(w_p/\rho_p)/\sum w_p\mu_p$, where I_p is the diffraction intensity from component p, w_p is the weight fraction of p, K_p is a constant which depends upon the inherent properties of p, the reflection being used, and the experimental arrangement, ρ_p is the density of p, and $\sum w_p\mu_p$ is the average attenuation coefficient [9]. In the case of polymorphic binary mixtures both phases have the same

mass attenuation coefficient, therefore the equation simplifies to $I_p/I_{p0} = w_p$, where I_{p0} is the diffraction intensity for the pure p phase. Although the theoretical correlation between the measured intensity of characteristic reflection and weight fraction of the phase is simple, there are numerous factors which have to be considered in a reliable analytical application. Based on theoretical considerations [9], a thorough review discussed 33 parameters that affect accuracy of quantitative analysis by XRPD [41]. These originate from the instrument, from the analyte and from the sample preparation; and the most important factors are the crystallite size, the preferred orientation and the sample preparation. The crystallite (coherent diffraction domain) size is critical for primary and secondary extinction, as well as microabsorption. Supposing it is usually unlikely that molecular crystals have a very high degree of perfection, and linear absorption coefficients of polymorphs are almost the same, extinction and microabsorption effects, wittingly or not, are commonly neglected. However, if the sample measured contains greater particles than a critical value, nonlinear effects may occur from the above cited equation due to absorption. This maximum acceptable particle size is $t_{max} = 1/100\mu$, μ being the average linear absorption coefficient [9]. Since organic crystals often have platy or acicular habits, another very serious problem can be the preferred orientation. As grinding can cause amorphisation and polymorph transitions in pharmaceuticals [42], in some cases there is no method to eliminate either absorption problems or preferred orientation. If the particles are always oriented in specific way, it can be advantageous to facilitate this orientation to decrease the random variation; for instance by applying pressure during filling the sample holder [10]. This approach, however, entrains the risk that the analytical method will only be accurate for measuring samples with similar properties, especially with the same particle size range; also stressed by others [12].

Famotidine form A grows as prismatic, while form B as acicular crystals. The particle size of the majority of form A crystals used for the preparation of calibration mixtures were in the range of 10–100 μm, but there were also present particles greater than 100 μm. Form B consisted of mostly 5–10 μm × 40–50 μm needles; none of them being longer than 100 μm (see Fig. 1). One aim of the study was to assess the possibility of constructing proper quantitative XRPD method for samples in their natural state, i.e. "as received". Therefore to avoid changing the properties of the substance in the first series of measurements the particle size problems were neglected. In a second series the samples were ground in agate mortar with a pestle, paying attention to mill the same amount of substance, with the same force, precisely for 3 min. Grinding significantly decreased the particle size of the crystals, as well as fractured them to be more isomorphous. The majority of the particles of both ground samples were less than 10 μm (Fig. 1).

Fig. 2 shows the XRPD patterns of famotidine polymorphs before and after grinding. In line with our previous results [38] the applied grinding did not induce polymorph transition. The pattern of form A did not change significantly, but the relative intensities of form B altered considerably. This is an indication of decreased preferred orientation. On the other hand, the absolute intensity of almost every reflection reduced, resulting in decreased total diffracted intensity. This could be the consequence of increased number of defect sites. According to [37], the average linear absorption coefficient of famotidine is 48.65 cm^{-1}, thus the maximum acceptable particle size for quantitative analysis would be 2.1 μm. This limit could not be attained with the applied grinding, and keeping in mind the likelihood of amorphisation of form B, the possibility of further grinding was excluded.

The relative standard deviation (R.S.D.) of form A reflection intensities, which seem to be the most appropriate for quantification (at 14.1 + 14.4°, 18.7° and 21.4° 2θ), were 20–40%, as determined from three measurements. This is unacceptable for quantitative analysis. Specific form B intensities (11.6°, 18.0° and 22.8° 2θ) varied only by 4–11%, which can be considered satisfactory. Grinding significantly decreased the intensity variation in both cases; it was 4–12% for form A, and less than 4% for form B in ground samples. It was inferred therefore that the variation originated basically from preferred orientation.

Reflections at 11.6° and 18.7° 2θ showed the smallest intensity variation and their intensities were plotted against the weight frac-

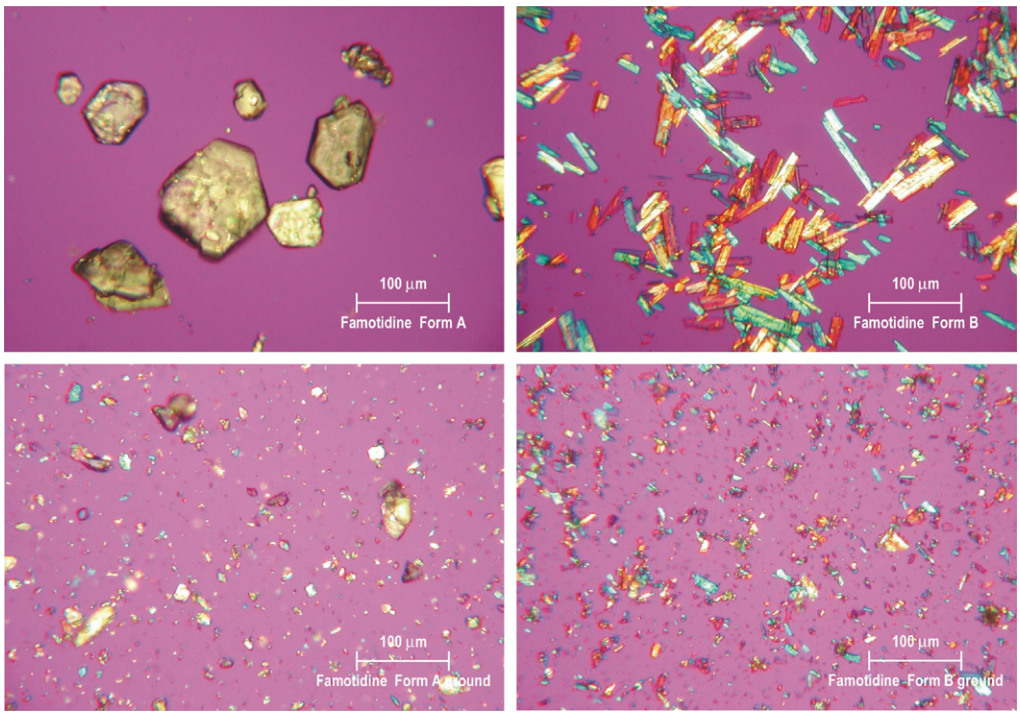

Fig. 1. Micrographs of form A (left on the top), form B (right on the top), ground form A (left on the bottom) and ground form B (right on the bottom) of famotidine.

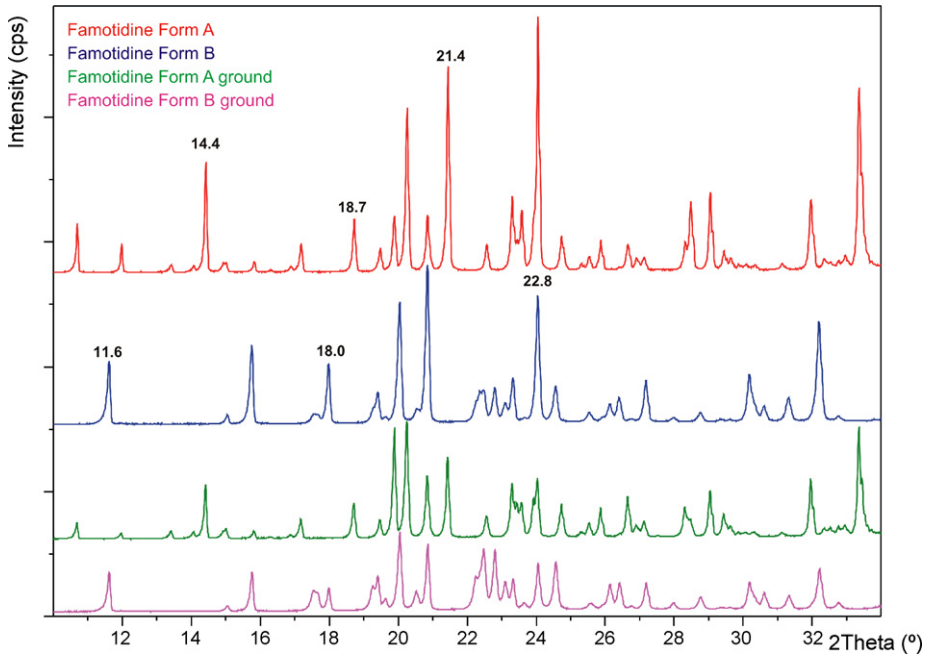

Fig. 2. X-ray powder diffraction patterns of form A and form B of famotidine, as well as ground form A and ground form B, from top to bottom, respectively.

tion to construct a univariate calibration correlation. This resulted in a straight line but with a low correlation coefficient, because of high scatter around the calibration line. The linear fit for the peak intensities measured on ground samples was much better, but in the case of form A there was still a relatively large scatter in the mixtures containing high percentage of form A. Likely source of this high variation may be the irreproducibility of sample filling procedure, which can lead to a difference in sample porosity in the surface region, and especially to composition dependent preferred orientation. Both can be handled by taking the ratios of proper reflection intensities. This is one reason why internal standards are commonly used in XRPD. However, increasing the number of components makes it more difficult to prepare homogeneous calibration mixtures, and also considerably increases sample preparation time when the method is applied on a routine basis; thus it was avoided. If only the two phases to be quantified are present in the sample, one may take the ratio of reflection intensities characteristic of different forms. For instance, if I_a and I_b are the intensities of reflections specific for form A and form B, respectively, the ratio $I_b/(I_b + I_a)$ gives linear correlation with concentration of form B, and this relationship has already been used for simple quantitative determination of polymorphic forms [17]. However, the correlation is linear only in that case when the corresponding intensities of pure phases, i.e. I_{a0} and I_{b0}, are the same. Otherwise the difference has to be taken in correction, and the equation changes to $I_b/(I_b + I_a(I_{b0}/I_{a0}))$. Regarding famotidine polymorphs, the integrated intensities of 11.6° and 18.7° 2θ reflections were selected, which were statistically not different in ground samples. The calibration lines are shown in Fig. 3 (considering that intensity ratios were used, the respective correlation for form A is essentially the same). The result is a linear correlation for the whole concentration range, with high coefficient and satisfactorily low standard deviation for repeated measurements. The variation was significantly lower in ground samples, again confirming the fact that grinding was advantageous in decreasing the preferred orientation and/or absorption problems.

The limit of detection (LOD) and quantitation (LOQ) were estimated as 3.3 and 10 times the standard deviation of blank divided by the slope of the calibration curve [43], respectively; with the modification that instead of blank (corresponding pure form) the 3% mixtures, expected to be close to the detection limit, were used, which were measured five times. The measured mean val-

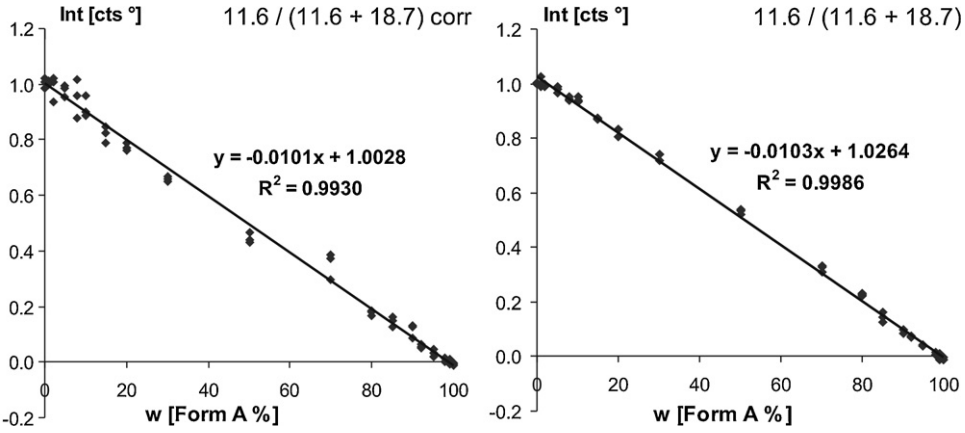

Fig. 3. Calibration correlation for famotidine form B XRPD data: samples measured "as received" (left) and after grinding (right). The ordinate is the ratio of the intensity at 11.6° 2θ to the sum of the intensities of 11.6° and 18.7° 2θ reflections; the correction factor is the intensity ratio determined for pure forms.

Table 1
Limits of detection and quantitation of univariate and multivariate XRPD methods.

	Univariate method				Multivariate method (PLS)			
	"As received"		Ground		"As received"		Ground	
	Form A	Form B	Form A	Form B	Form A	Form B	Form A	Form B
Predicted concentration of 3% mixtures (wt.%)	2.5	2.5	4.0	2.6	3.4	4.1	1.8	4.0
LOD (wt.%)	6.2	1.9	1.3	2.4	1.9	1.4	2.1	2.0
LOQ (wt.%)	18.9	5.8	3.9	7.2	5.9	4.2	6.2	6.0

ues indicative of the model accuracy, and the determined LOD and LOQ are shown in Table 1. The 6.2% LOD for form A in unground ("as received") samples is very high; however, it should be noted that visual inspection of characteristic reflections permits detection of ca. 3%. LOD for other cases is around 2%; and the observable bias in the calculated percentage of minor component from the 3% confirms that the LOQ values are higher than 3%.

Multivariate calibrations were performed on the 10.0–32.5° 2θ range excluding only the form A reflection at 33.4° 2θ which exhibited extraordinary intensity variation. There was no common reflection of famotidine polymorphs with similar intensity, which could have served as a normalization factor. The total diffracted intensity, as determined by integrating the area under the curve over the 10–34° 2θ range, after linear background correction was, however, independent of the composition. This quantity was used, therefore, to correct for absolute intensity variation. Ground samples did not fulfil this concentration independency as the ground form B had a bit lower total diffracted intensity than form A. Normalization, however, improved the calibration model in every case.

CLS models gave very poor results, but using PCR and PLS similarly good correlation was obtained. Mean centring and variance scaling were needed as preprocessing procedures. Data smoothing improved the models, but not significantly. Unexpectedly first derivatives of the diffractograms proved to be better input data than diffractograms itself, and smoothing was also advantageous. The results are shown in Tables 2 and 3. Multivariate data analysis on integrated intensities of some characteristic peaks which showed the least intensity variation in repeated measurements was also performed; this, however, gave slightly worse results than using every data point. Optimal number of principal components was determined by finding the minimum of RMSECV values in a leave-out-one cross-validation, or finding the minimum RMSEP if the previous did not gave unequivocal solution. Visual inspection of residual plot was employed to ascertain whether the difference between predicted and nominal concentration after cross-validation is randomly distributed around zero and independent of concentration.

PLS models built on smoothed 1st derivative data (typed bold in the tables) were selected as the best for both "as received" and ground samples, because of high correlation coefficient, low error values, and random distribution of residuals. Models explained about 90 and 95% of the signal variation by one factor, and this first principal component was identical with the difference of form A and form B diffractograms.

LOD and LOQ for the multivariate method were estimated from the standard deviation of the mixtures containing 3% of form A and 3% of form B, both measured five times, taking the predicted vs. nominal concentration as the calibration curve with unity slope (Table 1). Results are similar to that of calculated from univariate calibration; the detection and quantitation of form A, however, much better by multivariate data processing. This was expectable, because a method that takes into account the whole diffraction pattern is less sensitive for preferred orientation than that use individual reflection intensities.

3.2. Raman spectrometry

The quantitative analytical application of Raman spectroscopy is based on a modified version of the Lambert–Beer law. In a simplified form it is $I_\nu = I_0 K_\nu x$, where I_ν is the measured intensity of the Raman line of the scattering species at ν, I_0 is the intensity of the excitation laser line, ν is the Raman shift, x is the mole fraction of the species, and K_ν describes the overall spectrometer response, the self-absorption and molecular scattering properties of the medium, which can be assumed as a constant providing that instrumental factors do not change [25]. Comparing the Raman spectra of form A and form B of famotidine, it is clear that the polymorphs have distinct vibrational frequencies and relative band intensities, which may serve for unequivocal identification (Fig. 4). The most prominent differences are in the region of C–H stretching vibrations around 2900 cm^{-1} and in the region of bond deformation vibrations at 760–500 cm^{-1}. Unique bands of form A and form B are located at 658 cm^{-1} and 739 cm^{-1} respectively, which are free from spectral overlap and thus appropriate for univariate calibration.

Table 2
Performance characteristics of chemometric models built on "as received" famotidine XRPD data.

Method	Univariate	Diffractogram[a]		1st d[b]		1st d sm[c]	Area[d]
	Int. ratio	PCR	PLS	PCR	PLS	PLS	PLS
r	0.9965	0.9995	0.9996	0.9996	0.9999	**0.9997**	0.9990
RMSEC	5.988	1.270	1.090	1.120	0.686	**1.010**	1.760
RMSECV		1.820	1.780	1.600	1.530	**1.700**	1.970
RMSEP	3.468	1.270	1.200	1.290	1.260	**1.490**	1.910
CV residuals[e]	+	+	+	+	+	**+**	+
No. of factors		7	6	9	3	**3**	3
% PC1[f]		85.18	85.18	70.98	70.98	**89.12**	97.27

[a] 10.0–32.5° 2θ range.
[b] 1st derivative of the diffractogram.
[c] 1st derivative of the diffractogram after smoothing with Norris derivative filter (segment length = 17, gap = 2).
[d] Integrated intensity of specific peaks at 11.6°; 14.4°; 18.0° and 18.7° 2θ.
[e] "+" mark means that the distribution of the residuals in the function of concentration on the cross-validation plot is random around zero and "–" means not random distribution (curvature was observed).
[f] The percentage contribution of first principal component to the spectral variation in the selected range.

Table 3
Performance characteristics of chemometric models built on ground famotidine XRPD data.

Method	Univariate	Diffractogram[a]		1st d[b]		1st d sm[c]	Area[d]
	Int. ratio	PCR	PLS	PCR	PLS	PLS	PLS
r	0.9993	0.9997	0.9997	0.9995	0.9995	**0.9997**	0.9992
RMSEC	3.916	1.050	0.974	1.270	1.240	**1.050**	1.650
RMSECV		1.380	1.400	1.380	1.380	**1.450**	1.900
RMSEP	3.699	1.270	1.340	1.130	1.130	**1.060**	1.690
CV residuals[e]	+	–	–	+	+	**+**	+
No. of factors		4	3	1	1	**2**	3
% PC1[f]		92.39	92.39	84.77	84.77	**94.36**	95.76

[a] 10.0–32.5° 2θ.
[b] 1st derivative of the diffractogram.
[c] 1st derivative of the diffractogram after smoothing with Norris derivative filter (segment length = 9, gap = 2).
[d] Integrated intensity of specific peaks at 11.6°; 14.4°; 18.0°; 18.7° and 21.4° 2θ.
[e] "+" mark means that the distribution of the residuals in the function of concentration on the cross-validation plot is random around zero and "–" means not random distribution (curvature was observed).
[f] The percentage contribution of first principal component to the spectral variation in the selected range.

It was found that absolute Raman intensity of the same sample usually varied by about 8%, and in some mixtures the relative standard deviation of absolute intensity was more than 25%. Spectra were collected from the same sample holder, where the powder was roughly equally compact with about 4 mm thickness proved that practically infinite for the excitation beam used. Sample positioning error can be neglected because of auto focusing before every measurement. Repeating the measurements on different days from the same position by leaving the sample in the spectrometer, the intensity variation was negligible (<1%), indicating superior spectrometer stability. The observed absolute intensity variation, therefore, can originate from refraction and polarization effects, because of not equally random orientation of crystallites in different sampled positions. It is worth to note, however, that relative intensity variations of spectral bands, which could not be easily controlled by simple normalization, were not experienced. In this case the analysis needs only a proper quantity to normalize the spectra; and this can be the intensity of a relatively significant band in a spectral range common in both polymorphs. The peaks at 1330 cm^{-1} and 1333 cm^{-1}, characteristic for form A and form B, respectively, are appropriate for this purpose, since their intensity is similar for both forms. Normalization was carried out as a path length correction by TQ Analyst software taking the peak height after two point baseline correction.

Univariate calibration was performed on the integrated intensities of above mentioned characteristic peaks (after two point baseline correction), i.e. at 658 cm^{-1} and 739 cm^{-1} for form A and form B, respectively. After some repeated measurements on polymorphic mixtures, relatively high variation was found for predicted concentration, especially for mixtures containing low percentage of either form A or form B. It was inferred that samples were subsampled by the small laser spot therefore the analysed fraction was not representative of the bulk composition. To avoid this, average spectra were collected for every sample using different positions of the sample holder (see Section 2.4) and measurement procedure similar to that described in our other study [40]. Accumulating only four scans from a single point gave spectrum with acceptable signal-to-noise ratio, while about 6 mm^2 grid size seemed to be large enough sampled area and raising the numbers of point in the grid did not improve the statistics. On spectral data, collected with this measurement procedure, excellent linear correlation was obtained with low RMSEC, RMSECV as well as RMSEP; the residuals were randomly distributed around zero and the model explained 95% of full spectral variation in spite of that it utilized only two

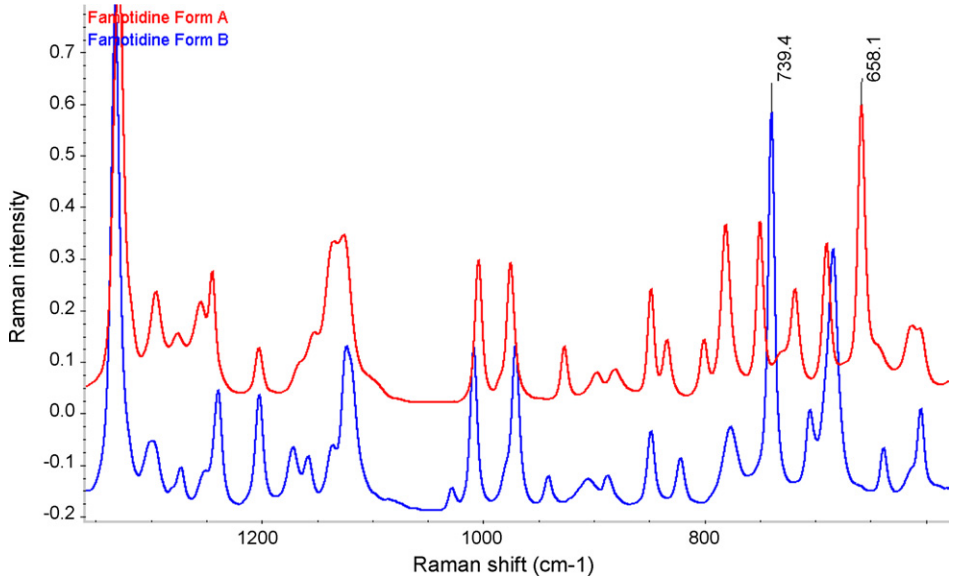

Fig. 4. The distinct FT-Raman spectral range of form A (red upper) and form B (blue lower) of famotidine.

Table 4
Limits of detection and quantitation of univariate and multivariate Raman methods.

	Univariate method				Multivariate method (PLS)	
	Int. vs. conc.[a]		Pred. vs. nom.[b]			
	Form A	Form B	Form A	Form B	Form A	Form B
Predicted concentration of 3% mixtures (wt.%)	3.1	3.3	3.1	3.3	3.1	3.0
LOD (wt.%)	2.6	0.9	2.5	0.8	1.2	0.9
LOQ (wt.%)	7.8	2.6	7.6	2.5	3.7	2.8

[a] Estimation from the measured Raman intensity vs. nominal concentration equation for the characteristic peak of form A and form B.
[b] Estimation from the predicted vs. nominal concentration correlation.

band intensities (Table 5). The intensity vs. concentration equations were $y = 0.0584x + 0.1078$ and $y = 0.0494x + 0.0184$ for form A and B, respectively; where y is the normalized Raman intensity and x is the wt.% of the corresponding form.

The limit of detection and quantitation were estimated in a similar way as in the case of XRPD, taking 3.3 and 10 times the standard deviation of the 3% mixtures from five measurements and dividing it by the slope of the calibration curve. The calculation was also done for the predicted vs. actual concentration curve calculated by TQ Analyst based on the simple Lambert–Beer algorithm with the slope of unity. The measured mean values, indicative of model accuracy, and the determined LOD and LOQ are shown in Table 4. Both methods used for the calculation of limits resulted in practically the same. LOD and LOQ for form A are significantly higher than for form B. This can also be observed by visual inspection of the mixtures containing 3% of form A and 3% of form B. There is no visible band due to form B on the spectrum of the 3% mixture, while the same percentage of form A appears as a weak band at 658 cm^{-1}. In spite of this, repeated measurements show no visible variation in the spectral intensities in the integration region around 739 cm^{-1}, while the intensity of 658 cm^{-1} band has apparent variation. The possible reason is the worse homogeneity of samples containing low percentage of form A compared to the rest of calibration mixtures; and this can be the consequence of its larger particle size which makes the mixing more difficult.

Multivariate calibrations were performed on the whole measured spectral range and its derivatives as well as on selected ranges and their derivatives. Table 5 summarizes the results. Normalization on the baseline corrected peak height of 1330–1333 cm^{-1} band proved to be the best preprocessing operation; multiplicative signal correction (MSC) and standard normal variate (SNV) gave slightly worse results. Mean centring was necessary to obtain good linear correlation, but variance scaling decreased model performances. PLS method slightly outperformed CLS and PCR models in every case. Models using the full spectral data seemed to be accurate and precise but the residuals had a bit curved distribution, which might indicate problems with robustness. Omitting useless spectral ranges, 2880–1700 cm^{-1} containing only noise, did not improve the model significantly. However, selecting the ranges most indicative of spectral differences of the two polymorphs lower RMSEC and RMSEP values were achieved by only one factor. In this case 1st and 2nd derivative spectral ranges gave better results, where the residuals have also a random narrow distribution around zero.

PLS model built on the 1st derivative of 2904–2889 cm^{-1}, 763–732 cm^{-1} and 668–648 cm^{-1} spectral ranges was selected as the best one, because of high correlation coefficient, low error values, and random distribution of residuals. This model explained 99% of the full spectral variation by one factor, in spite that it was constructed from very limited portion of spectral information. The first principal component was identical with the difference spectrum of form A and form B, thus confirming the adequacy of the model.

LOD and LOQ for both forms by the best multivariate method were estimated from the standard deviation of the mixtures containing 3% of form A and 3% of form B, respectively. The mixtures were measured five times and the predicted vs. nominal concentration correlation was considered as the calibration curve (Table 4). Multivariate analysis gave similar limits as Lambert–Beer method; however, in this case the LOD and LOQ for form A were significantly lower. It is supposed therefore that the higher limits of form A obtained in the univariate case are not only originated from worse sample mixing but also from inaccurate intensity determination of 658 cm^{-1} band at low concentration, which affects PLS method less.

The robustness of Raman methods against particle size variation was investigated through the quantification of ground samples by the calibration method obtained from “as received” samples. Among others, ground mixtures containing 3% of form A and 3% of form B were analysed five times. It was previously shown [40] that in the sampling accessory used in this study the measured intensity may be independent of the particle size. In the case of famotidine samples absolute intensity of both “as received” and ground samples varied by about 6% as measured by the spatially averaging procedure. The absolute intensities were about 10% higher for ground than for “as received” samples in both mixtures showing significant increase by decreasing particle size. The exact cause of this observation was not investigated; it is assumed, however, that not only the size of the scattering particles changed by grinding, but also the compactness of the sample, which was achieved during filling the sample in the sample holder. Changing the porosity of the scattering media may also influence the absolute Raman intensity, and the effect is probably dependent on the particle size. Nevertheless, the methods are based on normalized intensities, and as it was already discussed, these are independent of particle size. Lambert–Beer method resulted 2.7 (0.8)% form A and 3.4 (0.2)% form B, while PLS method gave 2.2 (0.9)% form A and 2.9 (0.3)% form B for the mixtures containing 3% of form A and form B, respectively. Numbers in parenthesis are standard deviations, and these also confirm that the determined LOD and LOQ for different methods are reasonable; and these are lower for form B.

3.3. Comparing X-ray powder diffractometry and Raman spectrometry

In order to assess the validity of the developed XRPD and Raman methods, these were tested on polymorphic mixtures of unknown composition, which were prepared by precipitation of famotidine under various conditions. These mixtures had different particle size and crystal habit than those used for the construction of calibration models. As a consequence, two of them (sample 2 and especially sample 3) showed extraordinary preferred orientation in XRPD, thus the measured diffractograms showed completely different relative intensities than those characteristic for famotidine pure forms or calibration mixtures. On the contrary the Raman spectra of these unknown mixtures did not exhibit any distortion from the calibration samples, indicating that the technique is not sensitive to particle size and crystal habit of famotidine. Table 6 shows the composition of samples calculated from the univariate and multivariate XRPD and Raman methods. Regarding that any typical single intensity-based quantitative method is more reliable

Table 5
Performance characteristics of various chemometric models built on famotidine Raman data.

Method	Form A	Form B	FR[a] spectrum		FR 1st	MR[b] 1st	SR[c]	SR 1st		SR 2nd
	Lambert–Beer		PCR	PLS	PLS	PLS	PLS	PCR	PLS	PLS
r	0.9986	**0.9995**	0.9994	0.9995	0.9994	0.9994	0.9995	0.9994	**0.9994**	0.9993
RMSEC	2.115	**1.327**	1.410	1.300	1.420	1.420	1.210	1.400	**1.400**	1.460
RMSECV	2.543	**1.427**	1.820	1.550	1.580	1.580	1.490	1.560	**1.560**	1.630
RMSEP	1.968	**0.617**	0.703	0.701	1.100	1.110	0.616	0.838	**0.837**	0.824
CV residuals[d]	+	**+**	–	–	–	–	–	+	**+**	+
No. of factors			3	2	1	1	2	1	**1**	1
% PC1[e]	99.94	**99.94**	99.12	99.12	99.01	99.07	99.70	99.37	**99.37**	98.71

[a] Full measured spectral range (FR): 3500–200 cm^{-1}.
[b] Meaningful spectral ranges (MR): 3475–2280 cm^{-1} and 1700–220 cm^{-1}.
[c] Selected spectral ranges (SR): 2904–2889 cm^{-1}, 763–732 cm^{-1} and 668–648 cm^{-1}.
[d] "+" mark means that the distribution of the residuals in the function of concentration on cross-validation plot is random around zero and "–" means not random distribution (curvature was observed).
[e] The percentage contribution of first principal component to the spectral variation in the selected spectral range.

Table 6
Composition of unknown samples determined by XRPD and Raman spectroscopy.

	XRPD "as received"				XRPD ground				Raman			
	Int. ratio		PLS		Int. ratio		PLS		Lambert–Beer		PLS	
	% A	% B	% A	% B	% A	% B	% A	% B	% A	% B	% A	% B
Sample 1	**1.7**	98.3	**3.0**	97.0	**3.8**	96.2	**2.6**	97.4	**2.7**	93.4	**3.8**	96.2
Sample 2	60.4	**39.6**	70.2	**29.8**	65.0	**35.0**	66.8	**33.2**	73.2	**34.0**	68.8	**31.2**
Sample 3	74.3	**25.7**	65.3	**34.7**	92.3	**7.7**	88.2	**11.8**	91.8	**9.6**	91.9	**8.1**
Sample 4	**6.8**	93.2	**9.7**	90.3	**7.8**	92.2	**9.9**	90.1	**10.3**	92.0	**10.5**	89.5
Sample 5	**5.0**	95.0	**7.5**	92.5	**7.3**	92.7	**8.0**	92.0	**9.1**	91.6	**8.9**	91.1
Sample 6	**3.9**	96.1	**4.7**	95.3	**5.4**	94.6	**4.7**	95.3	**4.6**	92.3	**4.8**	95.2

in the lower concentration range, in Raman Lambert–Beer method less than 50% of form A should be determined from the calibration curve derived for form A band intensity, while more than 50% of form A from form B band intensity. Respective results were typed bold in Table 6, similar values for other methods were signed just for better comparison.

The composition determined by univariate and multivariate methods shows good correlation for both XRPD and Raman spectrometry. In addition, both techniques gave practically the same results except for samples 2 and 3. Not surprisingly, the preferred orientation in these samples strongly disturbs the powder diffraction method and results in false composition determined by either intensity ratio or multivariate calibration. Grinding the samples before analysis and using the calibration correlation based on ground samples, XRPD is in accordance with Raman results.

4. Conclusions

Both X-ray powder diffractometry and Raman spectrometry are applicable for the quantitative measurement of famotidine polymorphic forms in their mixtures. Because of the variable properties of the analyte (particle size and crystal habit, and their combination as preferred orientation), Raman spectroscopy can provide more accurate and precise results than XRPD. It is also less sensitive for sample preparation including the way as the mixtures are produced. The otherwise desirable focused laser spot is a considerable drawback of quantitative application of Raman spectroscopy. Rotation and/or movement of the sample holder [26], however, can prevent sub-sampling. The measurement procedure in this and our previous study [40], which utilizes spatial averaging, resolves the problem of sub-sampling also for several tens or even hundreds micron particles and permits automatization of data collection as well. The latter is advantageous both for calibration measurements and for routine analysis of large number of samples.

Although X-ray powder diffractometry provides satisfactory quantitative results on ground famotidine samples, it is inferior compared to Raman spectrometry. It must be stressed that the XRPD method could be certainly improved but only by different measurement procedure (using transmission geometry, for instance, to reduce the effect of preferred orientation), more sophisticated sample preparation, or improving the counting statistics by longer signal accumulation. However, these all would increase the gross time needed for the analysis. The accumulation time for Raman measurements, applied in this study, required 6.5 min. It was 15 min for XRPD, which also shows the advantage of Raman spectrometry for routine analysis in industrial practice.

In the case of famotidine polymorphs, though multivariate data analysis can provide better results than univariate one, if appropriate analytical signals (normalized spectral intensities in Raman, and peak ratios in XRPD) are selected, the difference is negligible.

Acknowledgements

The authors thank Katalin Berki for supplying pure famotidine polymorphic forms and mixtures of unknown composition as well as technical assistance of Zsuzsanna Hoffmann in Raman measurements.

References

[1] J.K. Haleblian, W.C. McCrone, J. Pharm. Sci. 58 (1969) 911–929.
[2] A.S. Raw, M.S. Furness, D.S. Gill, R.C. Adams, F.O. Holcombe Jr., L.X. Yu, Adv. Drug Deliv. Rev. 56 (2004) 397–414.
[3] Food and Drug Administration, Center for Drug Evaluation and Research, Guidance for Industry, ANDAs: Pharmaceutical Solid Polymorphism: Chemistry, Manufacturing, and Controls Information, June 2007, http://www.fda.gov/cder/guidance/index.htm.
[4] J. Bernstein, Polymorphism of Molecular Crystals, Clarendon, Oxford, 2002.
[5] Federal Trade Commission, Generic Drug Entry Prior to Patent Expiration: An FTC Study, July 2002, http://www.ftc.gov/os/2002/07/genericdrugstudy.pdf.
[6] T.L. Threlfall, Analyst 120 (1995) 2435–2460.
[7] H.G. Brittain (Ed.), Polymorphism in Pharmaceutical Solids, vol. 95, Marcel Dekker, New York, 1999.
[8] A. Zakrzewski, M. Zakrzewski (Eds.), Solid State Characterization of Pharmaceuticals, Assa International Inc., Danbury, Connecticut, USA, 2006.

[9] H.P. Klug, L.E. Alexander, X-ray Diffraction Procedures for Polycrystalline and Amorphous Materials, 2nd edn., Wiley, New York, 1974.
[10] R. Suryanarayanan, Pharm. Res. 6 (1989) 1017–1024.
[11] R. Suryanarayanan, C.S. Herman, Pharm. Res. 8 (1991) 393–399.
[12] D.E. Bugay, A.W. Newman, W.P. Findlay, J. Pharm. Biomed. Anal. 15 (1996) 49–61.
[13] D.B. Black, E.G. Lovering, J. Pharm. Pharmacol. 29 (1977) 684–687.
[14] N.V. Phadnis, R. Suryanarayanan, Pharm. Res. 14 (1997) 1176–1180.
[15] R. Surana, R. Suryanarayanan, Powder Diffr. 15 (2000) 2–6.
[16] S.N. Campbell Roberts, A.C. Williams, I.A. Grimsey, S.W. Booth, J. Pharm. Biomed. Anal. 28 (2002) 1149–1159.
[17] Z. Dong, E.J. Munson, S.A. Schroeder, I. Prakash, D.J.W. Grant, Pharm. Res. 19 (2002) 1259–1264.
[18] T. Okumura, M. Otsuka, J. Pharm. Sci. 94 (2005) 1013–1023.
[19] S.S. Iyengar, N.V. Phadnis, R. Suryanarayanan, Powder Diffr. 16 (2001) 20–24.
[20] V. Uvarov, I. Popov, J. Pharm. Biomed. Anal. 46 (2008) 676–682.
[21] W. Dong, C. Gilmore, G. Barr, C. Dallman, N. Feeder, S. Terry, J. Pharm. Sci. 97 (2008) 2260–2276.
[22] M.J. Pelletier, Appl. Spectrosc. 57 (2003) 20A–42A.
[23] D.E. Bugay, Adv. Drug Deliv. Rev. 48 (2001) 43–65.
[24] G.A. Stephenson, R.A. Forbes, S.-M. Reutzel-Edens, Adv. Drug Deliv. Rev. 48 (2001) 67–90.
[25] C.G. Kontoyannis, C.Ch. Bouropoulos, P.G. Koutsoukos, Appl. Spectrosc. 51 (1997) 64–67.
[26] F.W. Langkilde, J. Sjöblom, L. Tekensberg-Hjelte, J. Mrak, J. Pharm. Biomed. Anal. 15 (1997) 687–696.
[27] L.S. Taylor, G. Zografi, Pharm. Res. 15 (1998) 755–761.
[28] N. Al-Zoubi, J.E. Koundourellis, S. Malamataris, J. Pharm. Biomed. Anal. 29 (2002) 459–467.
[29] S.N. Campbell Roberts, A.C. Williams, I.M. Grimsey, S.W. Booth, J. Pharm. Biomed. Anal. 28 (2002) 1135–1147.
[30] C.M. Deeley, R.A. Spragg, T.L. Threlfall, Spectrochim. Acta 47A (1991) 1217–1223.
[31] A.M. Tudor, S.J. Church, P.J. Hendra, M.C. Davies, C.D. Melia, Pharm. Res. 10 (1993) 1772–1776.
[32] G. Jalsovszky, O. Egyed, S. Holly, B. Hegedűs, Appl. Spectrosc. 49 (1995) 1142–1145.
[33] D. Pratiwi, J.P. Fawcett, K.C. Gordon, T. Rades, Eur. J. Pharm. Biopharm. 54 (2002) 337–341.
[34] C.J. Strachan, D. Pratiwi, K.C. Gordon, T. Rades, J. Raman Spectrosc. 35 (2004) 347–352.
[35] B. De Spiegeleer, B. Baert, N. Diericx, D. Seghers, F. Verpoort, L. Van Vooren, C. Burvenich, G. Slegers, J. Pharm. Biomed. Anal. 44 (2007) 254–257.
[36] B. Hegedűs, P. Bod, K. Harsányi, I. Péter, A. Kálmán, L. Párkányi, J. Pharm. Biomed. Anal. 7 (1989) 563–569.
[37] G. Ferenczy, L. Párkányi, J.G. Ángyán, A. Kálmán, B. Hegedűs, J. Mol. Struct. (Theochem.) 503 (2000) 73–79.
[38] Z. Német, B. Hegedűs, Cs. Szántay Jr., J. Sztatisz, G. Pokol, Thermochim. Acta 430 (2005) 35–41.
[39] F. Tian, F. Zhang, N. Sandler, K.C. Gordon, C.M. McGovering, C.J. Strachan, D.J. Saville, T. Rades, Eur. J. Pharm. Biopharm. 66 (2007) 466–474.
[40] Z. Német, Á. Demeter, G. Pokol, J. Pharm. Biomed. Anal. 49 (2009) 32–41.
[41] V.J. Hurst, P.A. Schroeder, R.W. Styron, Anal. Chim. Acta 337 (1997) 233–252.
[42] H.G. Brittain, J. Pharm. Sci. 91 (2002) 1573–1580.
[43] Food and Drug Administration, Center for Drug Evaluation and Research, Guidance for Industry, ICH Topic Q2B. Validation of Analytical Procedures: Methodology, November 1996, http://www.fda.gov/cder/Guidance/1320fnl.pdf.